

Enhancement of low temperature electron mobility due to an electric field in an InGaAs/InAlAs double quantum well structure

© T. Sahu^{*¶}, S. Palo⁺, P.K. Nayak^{*}, N. Sahoo[◇]

^{*} Department of Electronics and Communication Engineering,
National Institute of Science and Technology,
Berhampur-761 008, Odisha, India

⁺ Department of ECE, Kalam Institute of Technology,
Berhampur, Odisha

^{*} Department of ECE, SMIT,
Berhampur, Odisha

[◇] Department of Electronic Science, Berhampur University,
Berhampur-760007, India

(Получена 11 сентября 2013 г. Принята к печати 20 февраля 2014 г.)

The effect of external electric field F on multisubband electron mobility μ in an $\text{In}_{0.53}\text{Ga}_{0.47}\text{As}/\text{In}_{0.52}\text{Al}_{0.48}\text{As}$ double quantum well structure is analyzed. We consider scatterings due to ionized impurities, interface roughness and alloy disorder to analyze μ . The variation of scattering mechanisms as a function of F for different structure parameters shows interesting results through intersubband interactions. For small well widths, the mobility is governed by interface roughness scattering. When two subbands are occupied, the effect of impurity scattering gets enhanced through intersubband interactions. Our results of enhancement in mobility as a function of F , can be utilized for low temperature devices.

1. Introduction

$\text{In}_{0.53}\text{Ga}_{0.47}\text{As}/\text{In}_{0.52}\text{Al}_{0.48}\text{As}$ quantum well structure, lattice matched to InP substrate, has continued to draw attention as a potential material for high speed electronic and optoelectronic devices [1–3]. A double quantum well structure is an interesting system which exhibits tunneling coupling in addition to quantum confinement effect. Variation in the structure parameters such as well width, barrier width and doping concentration changes the subband energy levels and wave functions of the quantum well. By varying the structure parameters the occupation of subbands can be changed. For such systems where there is more than one subband is occupied, intersubband interaction plays a major role on the electron mobility [4–7]. A great deal of work has been done to study the multisubband electron mobility as a function of structure parameters of the quantum well systems [6–10]. In recent years attempts have also been made to study the influence of electric field on the electron mobility in quantum well structures [11–15]. The electric field affects the potential profile of the quantum well structure. As a result the subband energy levels and wave functions are changed which emends the electron mobility.

In the present work we analyse the electric field induced changes in the multisubband electron mobility in an $\text{In}_{0.53}\text{Ga}_{0.47}\text{As}/\text{In}_{0.52}\text{Al}_{0.48}\text{As}$ double quantum well structure. We consider symmetric scattering potentials: (i) ionized impurity (imp) scattering from the symmetrically placed delta-doped layers in the side barriers, (ii) interface roughness (IR) scattering from all the interfaces of the structure and (iii) alloy disorder (AL) scattering from the

wells as well as the barriers of the structure. We analyze the enhancement in electron mobility due to the effect of the external uniform electric field F , applied perpendicular to the interface plane, mediated by intersubband interactions. The effect of F alters the symmetric scattering potentials into asymmetric ones resulting interesting effects. We adopt the random phase approximation to obtain the screening of the scattering potentials [6,7,10] and analyze the influence of the electric field F on the scattering mechanisms by taking different well widths. In case of narrow well widths, the mobility is dominated by the IR scattering. We show that as long as the lowest subband is occupied, the electric field F has negligible effect on the subband mobility. However, with increase in well width, the second subband level starts occupying and the mobility gets influenced by the imp-scattering in addition to IR-scattering through the intersubband effects. Application of the electric field F causes transition from double subband occupancy to single subband occupancy, resulting enhancement in mobility due to the suppression of the intersubband scattering. At large well widths, the influence of IR-scattering gets reduced. It is interesting to note that with increase in F , the mobility due to the alloy disorder scattering μ^{AL} decreases and no discontinuity in mobility is seen at the transition from double subband to single subband occupancy because of negligible contribution of the intersubband scattering rate matrix elements. Therefore the enhancement in mobility, induced by the electric field, is mainly governed by the IR- and imp-scatterings in narrow well widths and imp-scattering for larger well widths. Further we show that as the well width increases the enhancement in mobility occurs at a lower field F . Our results can be utilized for low field device applications.

[¶] E-mail: tsahu_bu@rediffmail.com

2. Theory

We consider an $\text{In}_{0.53}\text{Ga}_{0.47}\text{As}/\text{In}_{0.52}\text{Al}_{0.48}\text{As}$ double quantum well structure. The side barriers (InAlAs layers) are delta-doped with a layer of width d and concentration N_0 . The doping layers lie at a distance s from the corresponding interfaces. The wells (InGaAs layers) are of width w . The width of the central barrier is b . The both the wells and the central barrier are undoped. The electrons diffuse into the adjacent wells. The band bending occurs due to the electrostatic interaction of the diffused electrons and the ionized donors through the alignment of Fermi level in the system. The electrons are confined to two narrow strips separated by a thin central barrier forming a coupled two-dimensional electron gas 2DEG [4]. We obtain an analytical expression for the potential profile $V(z)$ along the growth direction, say z -axis, by solving the Poisson's equation and adopting variational trial wave function method [4,10]. We incorporated the conduction band offset, i.e., the potential barrier height V_b at the interfaces of the quantum well structure and also the effect of the external uniform electric field F in the potential energy profile of the structure. The bound subband energy levels E_n and wave functions $\Psi_n(z)$ are obtained numerically by using multistep potential method [10,16].

At temperature $T = 0$, the subband transport lifetime $\tau_n = \tau_n(E_{Fn})$ since only the electrons on the Fermi surface contribute to the transport. E_{Fn} is the Fermi level of the n th subband, $E_{Fn} = E_F - E_n$. The expression for multisubband transport life time τ_n can be derived using the Boltzmann equation [5,6] in which τ_n contains the intra-subband and inter-subband scattering processes. For lower subbands one can express them in simple forms [5,7,10]. For example for a single occupied band ($n = 0$):

$$\frac{1}{\tau_0} = B_{00}. \quad (1)$$

For double occupied bands ($n = 0, 1$):

$$\frac{1}{\tau_0} = \frac{(B_{00} + C_{01})(B_{11} + C_{10}) - D_{01}D_{10}}{(B_{11} + C_{10}) + (E_{F1}/E_{F0})^{1/2}D_{01}},$$

$$\frac{1}{\tau_1} = \frac{(B_{00} + C_{01})(B_{11} + C_{10}) - D_{01}D_{10}}{(B_{00} + C_{01}) + (E_{F0}/E_{F1})^{1/2}D_{10}}. \quad (2)$$

The intrasubband scattering rate matrix element B_{nm} and intersubband scattering rate matrix elements C_{nm} and D_{nm} are expressed in terms of the matrix elements of screened scattering potentials $V_{nm}^{\text{eff}}(q)$ as [10]

$$B_{nm} = m/(\pi\hbar^3) \int_0^\pi d\theta (1 - \cos\theta) |V_{nm}^{\text{eff}}(q_{nm})|^2,$$

$$C_{nm} = m/(\pi\hbar^3) \int_0^\pi d\theta |V_{nm}^{\text{eff}}(q_{nm})|^2,$$

$$D_{nm} = m/(\pi\hbar^3) \int_0^\pi d\theta \cos\theta |V_{nm}^{\text{eff}}(q_{nm})|^2, \quad (3)$$

$$q_{nl} = [k_{Fn}^2 + k_{Fl}^2 - 2k_{Fn}k_{Fl}\cos\theta]^{1/2}, \quad k_{Fn} = (2mE_{Fn}/\hbar^2)^{1/2}.$$

We consider non phonon scattering mechanisms i.e., ionized impurity scattering, interface roughness scattering and alloy disorder scattering. The screened ionized impurity potential can be written as [10]:

$$|V_{nm}^{\text{imp}}(q)|^2 = \frac{4\pi^2 e^4 N_0}{\epsilon_0^2 q^2} \times \left[\int_{-(b/2+w+s+d)}^{-(b/2+w+s)} dz_i \left| \sum_{n'm'} \epsilon_{nm,n'm'}^{-1}(q) P_{n'm'}(q, z_i) \right|^2 + \int_{(b/2+w+s)}^{(b/2+w+s+d)} dz_i \left| \sum_{n'm'} \epsilon_{nm,n'm'}^{-1}(q) P_{n'm'}(q, z_i) \right|^2 \right] \quad (4)$$

where

$$P_{n'm'}(q, z_i) = \int_{-\infty}^{\infty} dz \Psi_{n'}(z) \Psi_{m'}(z) e^{-q|z-z_i|}. \quad (5)$$

Similarly the screened alloy scattering potential and interface roughness scattering potential can be written as:

$$|V_{nm}^{\text{Al}}(q)|^2 = \sum_j [a_j^3 (\delta V_j)^2 x_j (1 - x_j) / 4] \times \int_j dz \left| \sum_{n'm'} \epsilon_{nm,n'm'}^{-1}(q) \Psi_{n'}(z) \Psi_{m'}(z) \right|^2, \quad (6)$$

$$|V_{nm}^{\text{IR}}(q)|^2 = V_b^2 \pi \Lambda^2 \Delta^2 e^{-q^2 \Lambda^2 / 4} \times \sum_{bi} \left| \sum_{n'm'} \epsilon_{nm,n'm'}^{-1}(q) \Psi_{n'}^*(z) \Psi_{m'}(z) |_{z=z_{bi}} \right|^2. \quad (7)$$

$\epsilon_{nm,n'm'}^{-1}$ is the inverse of the dielectric screening matrix which can be expressed within the random phase approximation (RPA) as [4–7,10]:

$$\epsilon_{nm,n'm'}(q) = \delta_{nn'} \delta_{mm'} + (q_s/q) F_{nm,n'm'}(q) \chi_{n'm'}^0(q), \quad (8)$$

where $q_s = 2me^2/\epsilon_0\hbar^2$, F is the Coulomb form factor and χ is the static electron density — density correlation function without electron-electron interaction [4].

The ionized impurity scattering occurs from the two delta-doped layers lying in the side barriers. The alloy disorder scattering is considered from the well (InGaAs) regions as well as the barrier regions (InAlAs). Summation j is over all the layers of the structure. a_j is the lattice constant, δV_j is the alloy scattering potential and x_j is the alloy fraction of the j^{th} layer. Δ is the mean height and Λ is the correlation length of the roughness of the interfaces. The interface roughness is assumed to exist equally in all the four interfaces of the structure [17], unlike the other quantum well structures where the roughness is assumed to be in the bottom interfaces i.e., substrate side [8,18]. Sum

over bi is over all the interface planes z_i . n' , m' are subband indices. In the present structure the scattering potentials Eqs (4, 6 and 7) are symmetric about the centre of the structure along the z -axis.

The transport subband mobility of an electron in the n th subband μ_n is related to the subband transport lifetime τ_n by $\mu_n(\varepsilon) = (e/m)\tau_n(\varepsilon)$. The mobility μ^S due to a certain scattering mechanism S can be written as [10]:

$$\mu^S = \frac{\sum_n (n_n \mu_n^S)}{\sum_n n_n} \quad (9)$$

where μ_n^S is subband mobility of an electron due to S ($=$ imp, IR, AL) type of scattering in the n^{th} subband. n_n is the 2D-electron density in that subband. Further the total mobility μ can be calculated using Matheasen's rule considering the contribution of all the scattering mechanisms.

3. Results and discussion

We calculate the electron mobility in an $\text{In}_{0.53}\text{Ga}_{0.47}\text{As}/\text{In}_{0.52}\text{Al}_{0.48}\text{As}$ double quantum well structure by applying uniform electric field F in kV/cm perpendicular to the interface plane i.e., along z -axis. We note that the results of mobility remain unaffected by reversing the direction of the field F because of the symmetric nature of the scattering potentials about the centre of the structure along the z -axis. We take the width of the doping layer $d = 10 \text{ \AA}$, the spacer layer width $s = 40 \text{ \AA}$, the central barrier width $b = 30 \text{ \AA}$ and the doping concentration $N_0 = 1 \cdot 10^{18} \text{ cm}^{-3}$. The barrier height of the structure $V_b = 520 \text{ meV}$. The effective mass of the electron m/m_0 and the static dielectric constant ε_0 for the well (InGaAs)/barrier (InAlAs) are 0.042/0.08 and 13.93/12.42 respectively. The interface roughness parameters $\Lambda = 60 \text{ \AA}$ and $\Delta = 1.7 \text{ \AA}$ [17]. The alloy disorder potential δV for the well (InGaAs) and the barrier (InAlAs) are 0.6 eV and 1.4 eV respectively [19].

In Fig. 1, we plot the results of mobilities due to imp-, IR- and AL-scatterings μ^{imp} , μ^{IR} , μ^{Al} and total mobility μ respectively as a function of the electric field F in kV/cm using Eqs (1), 2 and 9 for well width $w = 80 \text{ \AA}$. We note that the magnitude of μ^{Al} is almost one order more than that of μ^{imp} and μ^{IR} . For $F = 0$, two levels are occupied. At $F = 10 \text{ kV/cm}$ the second subband becomes unoccupied resulting an enhancement in mobility due to the absence of the intersubband scattering. As long as the second subband is occupied, the imp-scattering is more effective than the IR-scattering due to the greater influence of the intersubband interaction on the imp-scattering. However, when single subband is occupied, the contribution of intersubband interaction ceases causing predominance of the IR-scattering. In order to analyze the enhancement in mobility, we present the intrasubband and intersubband scattering rate matrix elements Eq. (3) as functions of the

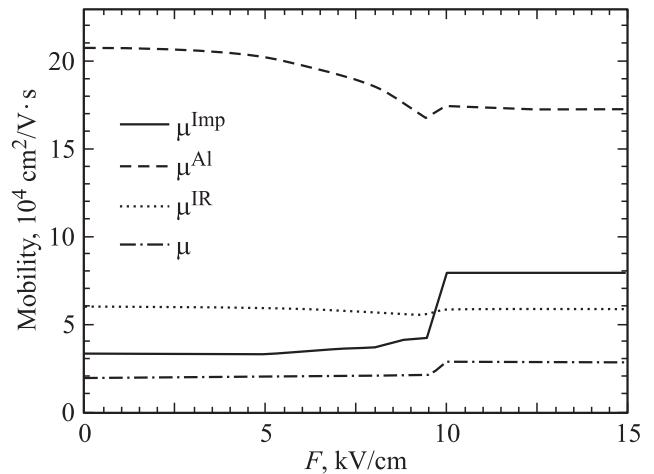


Figure 1. Electron mobility due to imp-, IR- and AL-scattering and total mobility as a function of the electric field F in kV/cm for $w = 80 \text{ \AA}$.

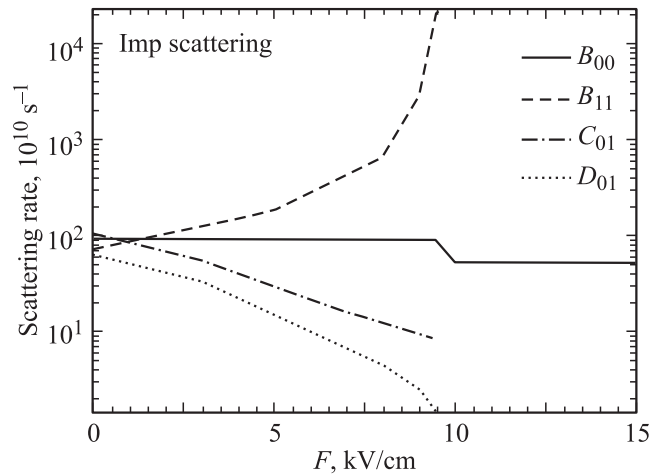


Figure 2. Intrasubband and intersubband scattering rate matrix elements for imp-scattering as a function of F in kV/cm for $w = 80 \text{ \AA}$.

electric field F in Fig. 2 for imp-scattering and in Fig. 3 for IR- and AL-scatterings. We note that the sudden enhancement in mobility at the transition from double subband occupancy to single subband occupancy is because of two factors: (i) change in the intrasubband scattering rate matrix element B_{00} through the discontinuity in the dielectric screening and (ii) absence of the additional intersubband scattering rate matrix elements C_{01} and D_{01} once single subband is occupied. From Fig. 2 we note that the change in μ^{imp} is mainly because of the sudden drop in B_{00}^{imp} . Whereas, no such discontinuity is seen in B_{00}^{IR} and B_{00}^{Al} (Fig. 3). The discontinuities in μ^{IR} and μ^{Al} (Fig. 1) are mainly due to the additional intersubband scattering rate terms C_{01} and D_{01} which cease when there is single subband occupancy. For IR- and AL-scatterings the magnitude of D_{01} is very negligible and hence it is not presented in Fig. 3.

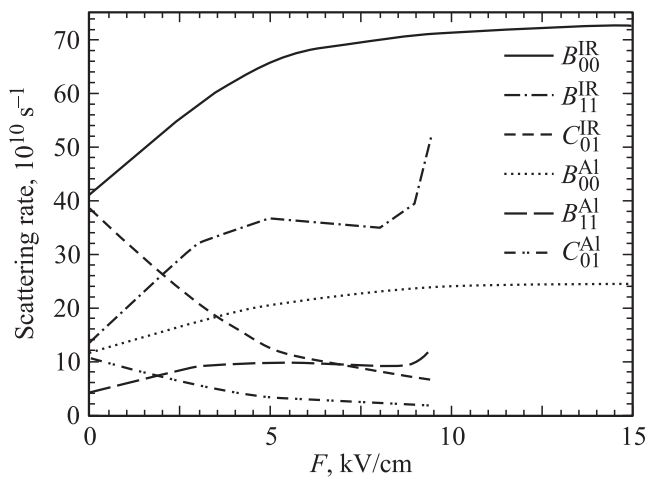


Figure 3. Intrasubband and intersubband scattering rate matrix elements for IR- and Al-scatterings as functions of F in kV/cm for $w = 80 \text{ \AA}$.

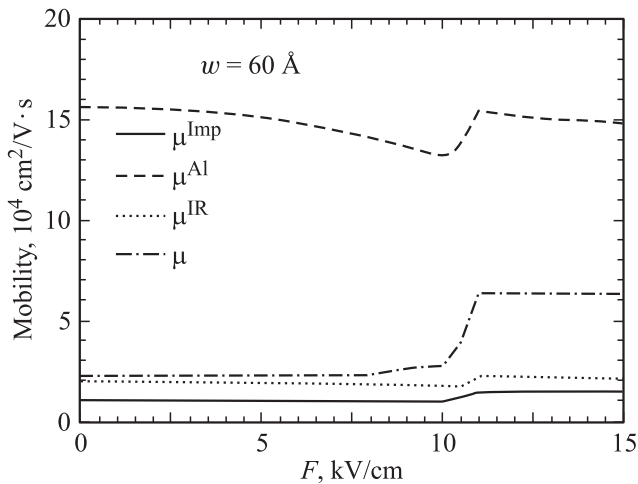


Figure 4. Mobility as a function of the electric field F for well width $w = 60 \text{ \AA}$.

We wish to study the effect of the electric field F on mobility by changing the well widths. In Figs. 4 and 5 we present μ^{imp} , μ^{IR} , μ^{Al} and μ taking well widths $w = 60$ and 120 \AA respectively. We note that for w less than 60 \AA (say 40 \AA), only the lowest subband is occupied and the mobility is dominated by the IR scattering. As the well width increases, say for $w = 60 \text{ \AA}$, as in Fig. 4, the second level is occupied at $F = 0$ and the imp-scattering influences the mobility more through intersubband interaction. As a result, the imp-scattering and IR-scattering almost equally influence the mobility. A sudden rise in mobility is obtained at the transition from double subband occupancy to single subband occupancy due to the suppression of the intersubband effects. Then the mobility is mostly influenced by the IR-scattering. With increase in w , say at $w = 80 \text{ \AA}$ (Fig. 1), the influence of imp- and IR-scatterings on mobility decreases unequally and as a result the difference between μ^{imp} and μ^{IR} becomes less μ^{imp} being greater

than μ^{IR} , so long as single subband is occupied. However, once double subband is occupied, the trend is reversed, $\mu^{\text{imp}} < \mu^{\text{IR}}$ due to the additional effect of the intersubband interaction. As w increases further (Fig. 5), the influence of IR-scattering becomes very less on mobility.

The influence of AL-scattering on mobility is interesting. Although it has a negligible contribution compared to other scattering mechanisms, the influence of AL-scattering on mobility enhances with increase in F . Furthermore, as the well width increases, the magnitude of sudden rise in μ^{Al} and μ^{IR} at the point of transition from double subband to single subband occupancy diminishes. In fact for $w = 120 \text{ \AA}$ there is almost no discontinuity in mobility. This is because of the fact that the intersubband scattering rate matrix elements C_{01} and D_{01} , which are comparable in magnitude with that of the intrasubband scattering rate matrix element B_{00} for small well widths (say, $w = 60 \text{ \AA}$), reduce to negligible values for large well widths (120 \AA)

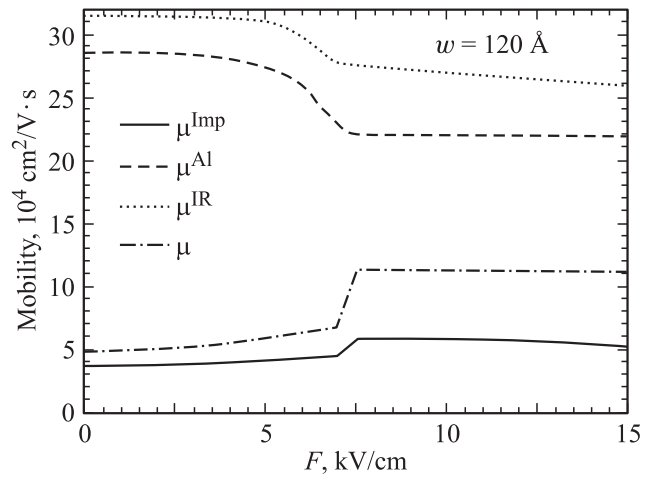


Figure 5. Mobility as a function of the electric field F for well width $w = 120 \text{ \AA}$.

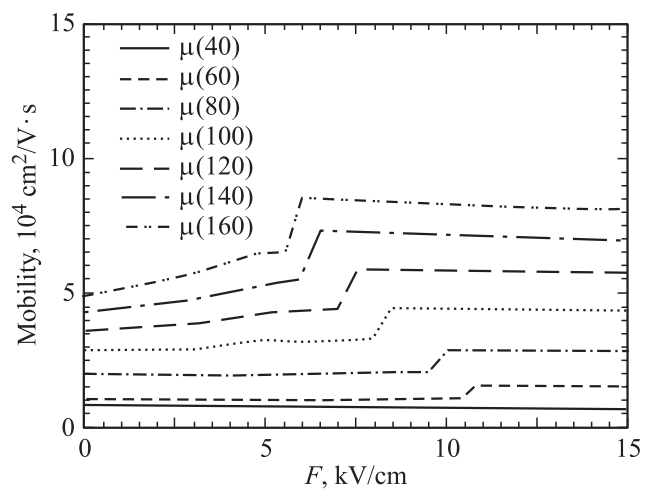


Figure 6. Comparison of total mobility μ as a function of electric field F for different well widths, $w = 40, 60, 80, 100, 120, 140$ and 160 \AA as written within the parenthesis in the figure.

near the point of transition from double subband to single subband occupancy. The continued drop in μ^{Al} and μ^{IR} are due to the continuous rise in B_{00} for AL- and IR-scatterings as seen from Fig. 3.

In Fig. 6, we present the total mobility μ as a function of the electric field F for different well widths, $w = 40, 60, 80, 100, 120, 140$ and 160 \AA . For $w = 40 \text{ \AA}$ single subband is occupied. For $w = 60 \text{ \AA}$ and onwards, two subbands are occupied at $F = 0$. Transition from double subband to single subband occupancy occurs at a field, say F_t , leading to enhancement of mobility due to containment of intersubband effects as discussed earlier. It is gratifying to show that the value of F_t decreases with increase in the well width. It would be interesting to compare our results of electric field dependent mobility with the experimental results when they will be available.

4. Conclusion

To summarize, we analyze the effect of external electric field on the low temperature multisubband electron mobility in an $\text{In}_{0.53}\text{Ga}_{0.47}\text{As}/\text{In}_{0.52}\text{Al}_{0.48}\text{As}$ double quantum well structure. We have considered non-phonon scattering mechanisms, viz., impurity scattering, interface roughness scattering and alloy disorder scattering. The influence of the electric field perpendicular to the interface plane alters the potential profile of the structure leading to changes in the electron subband energy levels and wave functions which affect the screened scattering potentials. With increase in the electric field the system undergoes transition from double subband to single subband occupancy resulting enhancement of mobility due to the absence of the intersubband effects. We analyse the changes in the electron mobility induced by the electric field by taking different well widths and show that for larger well widths the mobility enhances at a lower field. Our results of the mobility for the coupled quantum well structure can be utilized for low temperature device applications.

References

- [1] B.O. Lim, M.K. Lee, T.J. Baek, M. Han, S.C. Kim, J.K. Rhee. IEEE Electron Dev. Lett., **28**, 546 (2007).
- [2] M.P. Pires, C.L. De Souza, B. Yavich, R.G. Pereira, W. Caevalho. J. Light Wave Technol., **18**, 598 (2000).
- [3] Z. Xu, C. Wong, W. Qi, Z. Yuan. Optics Lett., **35**, 736 (2010).
- [4] T. Ando, A.B. Fowler, F. Stern. Rev. Mod. Phys., **54**, 437 (1982).
- [5] R. Fletcher, E. Zaremba, M.D. Iorid, C.L. Foxon, J.J. Harris. Phys. Rev. B, **41**, 10 649 (1990).
- [6] G.Q. Hai, N. Studart, F.M. Peeters. Phys. Rev. B, **52**, 8363 (1995).
- [7] T. Sahu, K.A. Shore. Semicond. Sci. Technol., **24**, 095 021 (2009).
- [8] S.K. Lyo. J. Phys. Condens. Matter, **13**, 1259 (2001).
- [9] J.M. Li, J.J. Wu, X.X. Han, Y.W. Lu, X.L. Liu, Q.S. Zhu, Z.G. Wang. Semicond. Sci. Technol., **20**, 1207 (2005).
- [10] P.K. Subudhi, S. Palo, T. Sahu. Superlat. Microstr., **51**, 430 (2012).
- [11] P.K. Basu, D. Raychaudhury. J. Appl. Phys., **68**, 3443 (1990).
- [12] F.M.S. Lima, A.L.A. Fonseca, O.A.C. Nunes. J. Appl. Phys., **92**, 5296 (2002).
- [13] T. Sahu, K.A. Shore. J. Appl. Phys., **107**, 113 708 (2010).
- [14] T. Sahu, S. Palo, N. Sahoo. Physica E, **46**, 155 (2012).
- [15] T. Sahu, N. Sahoo, A.K. Panda. Superlat. Microstr., **61**, 50 (2013).
- [16] Y. Ando, T. Itoh. J. Appl. Phys., **61**, 1497 (1987).
- [17] S. Tsujino, A. Borak, E. Müller, M. Scheinert, C.V. Falub, H. Sigg, D. Grutzmacher, M. Giovannini, J. Faist. Appl. Phys. Lett., **86**, 062 113 (2005).
- [18] K. Inoue, T. Matsuno. Phys. Rev. B., **47**, 3771 (1993).
- [19] A. Vasanelli, A. Leuliet, C. Sirtori, A. Wade, G. Fedorov, D. Smirnov, G. Bastard, B. Vinter, M. Giovannini, J. Faist. J. Appl. Phys. Lett., **89**, 172 120 (2005).

Редактор Т.А. Полянская